



# Cortical morphology in children and adolescents with different apolipoprotein E gene polymorphisms: an observational study

Philip Shaw, Jason P Lerch, Jens C Pruessner, Kristin N Taylor, A Blythe Rose, Deanna Greenstein, Liv Clasen, Alan Evans, Judith L Rapoport, Jay N Giedd

## Summary

**Background** Alleles of the apolipoprotein E (APOE) gene modulate risk for Alzheimer's disease, with carriers of the  $\epsilon 4$  allele being at increased risk and carriers of the  $\epsilon 2$  allele possibly at decreased risk compared with non-carriers. Our aim was to determine whether possession of an  $\epsilon 4$  allele would confer children with a neural substrate that might render them at risk for Alzheimer's disease, and whether carriers of the  $\epsilon 2$  allele might have a so-called protective cortical morphology.

**Methods** 239 healthy children and adolescents were genotyped and had repeated neuroanatomic MRI (total 530 scans). Mixed model regression was used to determine whether the developmental trajectory of the cortex differed by genotype.

**Findings** Cortical thickness of the left entorhinal region was significantly thinner in  $\epsilon 4$  carriers than it was in non- $\epsilon 4$  carriers (3.79 [SE 0.06] mm, range 1.54–5.24 vs 3.94 [0.03] mm, 2.37–6.11;  $p=0.03$ ). There was a significant stepwise increase in cortical thickness in the left entorhinal regions, with  $\epsilon 4$  carriers having the thinnest cortex and  $\epsilon 2$  carriers the thickest, with  $\epsilon 3$  homozygotes occupying an intermediate position (left  $\beta$  0.11 [SE 0.05],  $p=0.02$ ). Neuroanatomic effects seemed fixed and non-progressive, with no evidence of accelerated cortical loss in young healthy  $\epsilon 4$  carriers.

**Interpretation** Alleles of the apolipoprotein E gene have distinct neuroanatomic signatures, identifiable in childhood. The thinner entorhinal cortex in individuals with the  $\epsilon 4$  allele might contribute to risk of Alzheimer's disease.

## Introduction

In patients with Alzheimer's disease, the entorhinal cortex lying within the medial temporal lobe is the first brain region to show the characteristic pathology of the disease—neurofibrillary tangles—which can be found in individuals as young as 20 years.<sup>1–3</sup> In-vivo neuroimaging studies of patients with Alzheimer's disease delineate degenerative cortical changes sweeping from the entorhinal and medial temporal regions<sup>4–7</sup> to higher-order temporoparietal association cortices and then to frontal and finally primary sensorimotor and occipital areas.<sup>8–10</sup> Decreased entorhinal volume and hypometabolism predict the development of Alzheimer's disease both in healthy older adults and in those with mild cognitive impairment.<sup>11,12</sup>

The  $\epsilon 4$  allele of the apolipoprotein E (APOE) gene has emerged as the most robust genetic risk factor for the development of Alzheimer's disease.<sup>13,14</sup> Healthy adults with the  $\epsilon 4$  allele show altered patterns of brain activity both at rest and during cognitive challenges.<sup>15–20</sup> Although such studies establish the neurophysiological effects of APOE polymorphisms in healthy adults, whether there are any neuroanatomic correlates, especially in children, is less clear. Further, the  $\epsilon 4$  allele is also associated with deficits in core aspects of neuronal development and repair,<sup>21–24</sup> rendering carriers more susceptible to age-related neurodegeneration. Such subtle progressive

change might be noted even in children, again especially in regions where the earliest changes of Alzheimer's disease are found.

Just as the  $\epsilon 4$  allele has been implicated as a risk allele for neurodegenerative change, some studies find that  $\epsilon 2$  allele might have some protective qualities, since carriers have a lower risk of developing Alzheimer's disease.<sup>14,25–28</sup> Whether possession of the  $\epsilon 2$  allele might have different neuroanatomic effects to the  $\epsilon 4$  allele, which might partly explain the epidemiological findings, remains unexplored.

Our aim was thus to examine the possibility that possession of an  $\epsilon 4$  allele might confer children and adolescents with a neural substrate that renders them at risk for the development of Alzheimer's disease in later life. We might expect such structural differences to occur where the earliest changes of Alzheimer's disease arise—ie, the entorhinal and other medial temporal and orbitofrontal cortical regions.<sup>1–3,29</sup>

## Methods

### Participants

Unrelated children and adolescents aged 21 years or less with no personal or family history of psychiatric or neurological disorders were recruited mostly from the local community around Bethesda, MA, USA. The institutional review board of the National Institute of

Lancet Neurol 2007; 6: 494–500

Published Online

April 24, 2007

DOI:10.1016/S1474-

4422(07)70106-0

See Reflection and Reaction

page 471

Child Psychiatry Branch,  
National Institute of Mental  
Health, Bethesda, MD, USA

(P Shaw MD, K N Taylor BS,  
A B Rose BS, D Greenstein PhD,  
L Clasen PhD, J L Rapoport MD,  
J N Giedd MD); and Montreal  
Neurological Institute, McGill  
University, Montreal, Quebec,  
Canada (J P Lerch PhD,  
J C Pruessner PhD,  
Prof A Evans PhD)

Correspondence to:

Philip Shaw, 10 Center Drive,  
MSC1600, Building 10, Room  
3N202, Bethesda, Maryland  
20891-1600, USA  
shawp@mail.nih.gov

Mental Health approved the research protocol. Written informed consent and assent to participate in the study were obtained from parents and children, respectively.

### Procedures

For genotyping, PCR products were sequenced by pyrosequencing technology with two sequencing primers on the PSQ96 system (Biotage, Uppsala, Sweden) according to the manufacturer's instructions. The primers used were APO156 (5' CGATGACCTGCAGAA3') and APO112 (5' GACATGGAGGACGTG3'). The results were analysed with the PSQ96 SNP software.

For the first neuroanatomic analyses, the groups were split into  $\epsilon 4$  carriers and non- $\epsilon 4$  carriers. Individuals were then further divided into three groups:  $\epsilon 2$  carriers,  $\epsilon 3$  homozygotes, and  $\epsilon 4$  carriers. Individuals who had the  $\epsilon 2\epsilon 4$  genotype were excluded from the main analyses, as our hypothesis predicted opposing neuroanatomic effects of the  $\epsilon 2$  and  $\epsilon 4$  alleles. Details are discussed in webappendix 1.

All images were acquired with the same 1.5-T Signa MRI scanner (General Electric, Milwaukee, WI, USA) with a 3D spoiled gradient recall acquisition in the steady state (5 ms time to echo, 24 ms time to repeat, 45° flip angle, one repetition; 24 cm<sup>2</sup> field of view). T1-weighted images with contiguous 1.5 mm slices in the axial plane in thickness (124 per brain) were obtained. The images were collected in a 192×256 acquisition matrix and were 0-filled in k space to yield an image of 256×256 pixels, resulting in an effective voxel resolution of 0.9375×0.9375×1.5 mm<sup>3</sup>. Further details of the scanning protocol, such as standardised head alignment, were described by Giedd and colleagues.<sup>30</sup> The native MRI scans were registered into standardised stereotaxic space with a linear transformation<sup>31</sup> and corrected for non-uniformity artifacts.<sup>32</sup> The registered and corrected volumes were segmented into white matter, grey matter, cerebrospinal fluid, and background with an advanced neural net classifier.<sup>33</sup> A surface deformation algorithm was applied which first fits the white matter surface and then expands outward to find the grey matter-cerebrospinal fluid intersection, defining a known relation between each vertex of the white matter surface and its grey matter surface counterpart; cortical thickness can thus be defined as the distance between these linked vertices (40 962 such vertices are calculated).<sup>34</sup> The white and grey matter surfaces were resampled into native space by inverting the initial stereotaxic transformation. We report in detail analyses done in native space<sup>34,35</sup> since these are closer to the real dimensions of the cortex than measurements made in standard space, but also describe the pattern of results in stereotaxic space. In estimating cortical thickness we chose a 30-mm-bandwidth blurring kernel on the basis of population simulations that indicated that this bandwidth maximised statistical power while minimising false positives.<sup>36</sup> This selection also preserves the capacity

for anatomical localisation since 30-mm blurring along the surface with a diffusion smoothing operator represents considerably less cortex than the equivalent volumetric Gaussian blurring kernel, because it preserves cortical topological features.<sup>36</sup>

Two upgrades were made to the scanner during the study. For each upgrade, 38 individuals were scanned twice shortly before the upgrade, and then twice again in the week following the upgrade. The intra-class correlations for all grey matter lobar volumetric measures between pairwise combinations of the before and after upgrade scans were greater than 0.96.

To investigate cortical thickness in the regions of interest, an experienced neuroanatomist (JCP) manually defined the entorhinal cortex on ten randomly selected scans from the sample by use of protocols for parcellation of the medial temporal lobe.<sup>37</sup> The outlined regions of interest from all individuals were then used to create customised paediatric maps, which were projected onto the standard brain template (webfigure 1 shows the regions of interest displayed on several individual patient surfaces, along with key landmarks). The cortical thickness of each region of interest was taken as the mean value of all vertices lying within the region of interest. Analyses were also done at the level of individual vertices. Finally, for regions outside the medial temporal regions of interest, a fully automated segmentation program was used to assign every vertex to a cortical region at a sublobar level.<sup>38</sup> This atlas was used to define the major lobes. For example, the cortical thickness of the frontal lobes was estimated as the mean of the

See Online for webappendices 1, 2, and 3 and webfigures 1, 2, 3, 4, and 5

|   | $\epsilon 4$ carriers         |                              | Non- $\epsilon 4$ carriers                                     |                                  |
|---|-------------------------------|------------------------------|--|----------------------------------|
|   | $\epsilon 3\epsilon 4$ (n=60) | $\epsilon 4\epsilon 4$ (n=5) | $\epsilon 2$ heterozygotes (all $\epsilon 2\epsilon 3$ , n=29) | $\epsilon 3$ homozygotes (n=145) |
| <b>Scan details</b>   |                               |                              |  |                                  |
| One scan  | 65 (100%)                     |                              | 29 (100%)  | 145 (100%)                       |
| Two scans   | 42 (65%)                      |                              | 17 (59%)   | 100 (69%)                        |
| Three scans   | 21 (32%)                      |                              | 12 (41%)   | 60 (41%)                         |
| Four or more scans  | 8 (12%)                       |                              | 5 (17%)  | 25 (17%)                         |
| <b>Age at scan</b>  |                               |                              |  |                                  |
| One scan  | 11.2 (3.6)                    |                              | 10.8 (4.0)   | 11.2 (3.6)                       |
| Two scans   | 13.1 (3.8)                    |                              | 11.5 (3.4)   | 13.3 (3.7)                       |
| Three scans   | 15.7 (3.8)                    |                              | 15.1 (4.7)   | 15.3 (3.6)                       |
| Four or more scans  | 18.0 (2.3)                    |                              | 18.9 (1.3)   | 16 (4.0)                         |
| <b>Demographic characteristics</b>  |                               |                              |  |                                  |
| Sex (male)  | 32 (49%)                      |                              | 16 (55%)   | 84 (58%)                         |
| Ethnic origin   |                               |                              |  |                                  |
| White   | 55 (85%)                      |                              | 25 (86%)   | 123 (85%)                        |
| Black   | 8 (12%)                       |                              | 1 (3%)   | 9 (6%)                           |
| Other   | 2 (3%)                        |                              | 3 (10%)  | 13 (9%)                          |
| IQ  | 112.6 (14.1)                  |                              | 113.1 (12.1)   | 112.7 (13)                       |
| Total brain volume (mL)   | 1157 (112)                    |                              | 1165 (132)   | 1180 (117)                       |
| Data are n (%) or mean (SD).  |                               |                              |  |                                  |
| <b>Table 1: Details of scan acquisition and demographic characteristics of groups</b> |                               |                              |  |                                  |

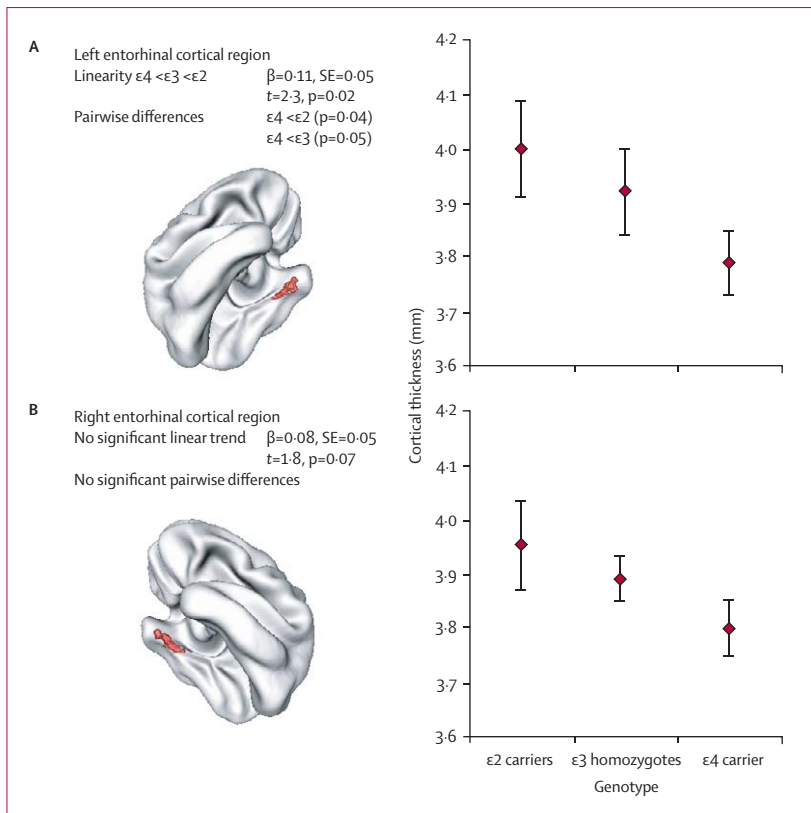


**Figure 1: Thickness of the entorhinal cortex by APOE genotype**  
The brain template (left) shows the region of interest; the graphs show the thickness of the cortex for each group.

See Online for webttables 1, 2 and 3

values for the superior, middle, inferior, postcentral, orbitofrontal, and cingulate gyri. The lateral temporal cortex was obtained as the mean cortical thickness of the superior and middle temporal gyri.

**Statistical analyses**

Mixed model regression was used for neuroanatomic analyses since it permits the inclusion of multiple measurements per person at different ages and irregular intervals between measurements, thereby increasing statistical power.<sup>39</sup> Initial analyses estimated group differences in mean cortical thickness both in the regions of interest and across the entire cortex, using a longitudinal model. Thus for the group comparisons, the

ith individual’s jth cortical thickness at a given vertex or region of interest was modelled as:

$$\text{Thickness}_{ij} = \text{intercept} + d_i + \beta_1(\text{group}) + \beta_2(\text{age} - \text{mean age}) + \beta_3(\text{group} * [\text{age} - \text{mean age}]) + e_{ij}$$

where  $d_i$  is a random effect modelling within-person dependence; the intercept and terms are fixed effects, and  $e_{ij}$  represents the residual error. Group differences in height, representing difference in cortical thickness, were determined by the significance of the  $\beta_1$  term. Group differences in the slope representing the trajectory of cortical change were determined by the significance of the interaction term,  $\beta_3$ . Graphs illustrating the developmental trajectories of the regions of interest were generated by use of fixed effects parameter estimates for the central 80% of the age range. The model applies only to the age range covered and cannot be extrapolated beyond this age range. Further details of the longitudinal analyses, including the rationale for adopting a linear model are given in webappendix 2 (see also webtable 1 and webfigure 2).

The group differences between  $\epsilon 4$  carriers and non-carriers in cortical thickness in the regions of interest were compared with cortical thickness estimated across the frontal, parietal, occipital, and inferolateral temporal cortices, neocortical regions where no structural effect of genotype was predicted. We postulated that there would be a linear effect of genotype, such that the  $\epsilon 2$  carriers would have the thickest cortex, followed by  $\epsilon 3$  homozygotes, and then finally  $\epsilon 4$  carriers. Initial analyses treating the group as an ordered factor showed that non-linear relations were not significant and the final model thus treated group as an interval variable (with  $\epsilon 2$  carriers=0,  $\epsilon 3$  homozygotes=1, and  $\epsilon 4$  carriers=2). The value of the  $\beta_1$  term for the group indicates whether the linear relation between the dependent variable (eg, the thickness of the entorhinal cortex) and the APOE genotype group was significant.

Analyses were also done at the level of individual cortical points, unconstrained by a priori regions of interest, generating  $t$  statistics that were visualised through projection onto a standard brain template.

For the entorhinal region of interest a significance level of  $p < 0.05$  was adopted. For analyses at the level of

|                                 | $\epsilon 4$ carrier   | Non- $\epsilon 4$ carrier | $\epsilon 4$ carrier vs non-carrier $t$ value | $p$  | $\epsilon 2$ carriers  | $\epsilon 3$ homozygotes | Pairwise differences between $\epsilon 2$ carriers, $\epsilon 3$ homozygotes and $\epsilon 4$ carriers         |
|---------------------------------|------------------------|---------------------------|---|------|------------------------|--------------------------|--|
| <b>L entorhinal region (mm)</b> | 3.79 (0.06; 1.54–5.24) | 3.94 (0.03; 2.37–6.11)    | 2.2   | 0.03 | 4.00 (0.07; 2.37–5.06) | 3.92 (0.04; 2.44–6.11)   | $\epsilon 4 < \epsilon 3$ $p=0.05$<br>$\epsilon 4 < \epsilon 2$ $p=0.05$<br>$\epsilon 3 < \epsilon 2$ $p=0.45$ |
| <b>R entorhinal region (mm)</b> | 3.80 (0.05; 2.15–5.83) | 3.90 (0.03; 2.39–5.33)    | 1.7   | 0.09 | 3.95 (0.08; 2.54–5.24) | 3.89 (0.04; 2.39–5.33)   | $\epsilon 4 < \epsilon 3$ $p=0.13$<br>$\epsilon 4 < \epsilon 2$ $p=0.11$<br>$\epsilon 3 < \epsilon 2$ $p=0.52$ |

Data are mean (SE; min–max).

**Table 2: Mean cortical thickness in the entorhinal and hippocampal regions of interest**

individual cortical points, group differences significant at an unadjusted  $p < 0.05$  are presented, in addition to those differences that remained significant after adjustment for multiple comparisons using the false discovery rate procedure (set at 0.05).<sup>40,41</sup> A false discovery rate threshold was determined for the statistical model using all  $p$  values pooled across all effects included in the model.

All analyses were repeated after confining the sample to the white, non-hispanic group only. To examine sex effects, the model parameters were initially allowed to reflect interactions between sex, genotype group, and age.

### Role of the funding source

The sponsor of the study had no role in study design, data interpretation, or writing of the report. The corresponding author had full access to all of the data in the study and PS, JLR, and JNG had final responsibility for the decision to submit for publication.

### Results

239 children and adolescents were recruited. 116 (49%) were singleton births and 123 (51%) were twin births. Only one child per twin set was included. 65 individuals were  $\epsilon 4$  carriers (60 heterozygotes with  $\epsilon 3\epsilon 4$  alleles, and five  $\epsilon 4$  homozygotes); 174 were non- $\epsilon 4$  carriers (29 with  $\epsilon 2\epsilon 3$  and 145  $\epsilon 3$  homozygotes). The groups were much the same in terms of demographic variables, IQ, and total brain volume (table 1). A similar proportion of individuals in each genotype group had repeated scan acquisitions, and those with single compared with repeated scans did not differ between genotype groups on baseline variables (webappendix 3 and webtable 2).

$\epsilon 4$  carriers had a significantly thinner cortex within the left entorhinal cortical region than did non-carriers. The cortex in the right entorhinal region was thinner in  $\epsilon 4$  carriers than in non-carriers, although this difference was not significant (figure 1 and table 2). There was a significant stepwise increase in the thickness of the left entorhinal cortex in the regions of interest, from the  $\epsilon 4$  carriers to the  $\epsilon 3$  homozygotes, and finally the  $\epsilon 2$  carriers.

Analyses at the level of individual cortical points showed that group differences (at an unadjusted  $p < 0.05$ ) between the  $\epsilon 4$  carriers and non-carriers were mainly in the medial temporal cortex, especially in the parahippocampal gyrus and uncus regions, extending posteriorly to the medial lateral occipitotemporal cortex and anteriorly to the postero-medial orbitofrontal cortex, where the group differences remained significant following adjustment for multiple comparisons (figure 2 and webfigure 3). In all the medial temporal and orbitofrontal regions, there was also a linear effect of genotype, with  $\epsilon 4$  carriers having a thinner cortex than  $\epsilon 3$  homozygotes, who in turn had thinner cortex than  $\epsilon 2$  carriers (webfigure 4). No differences were found throughout the remaining frontal, parietal, occipital, and lateral temporal cortex (webtable 3).

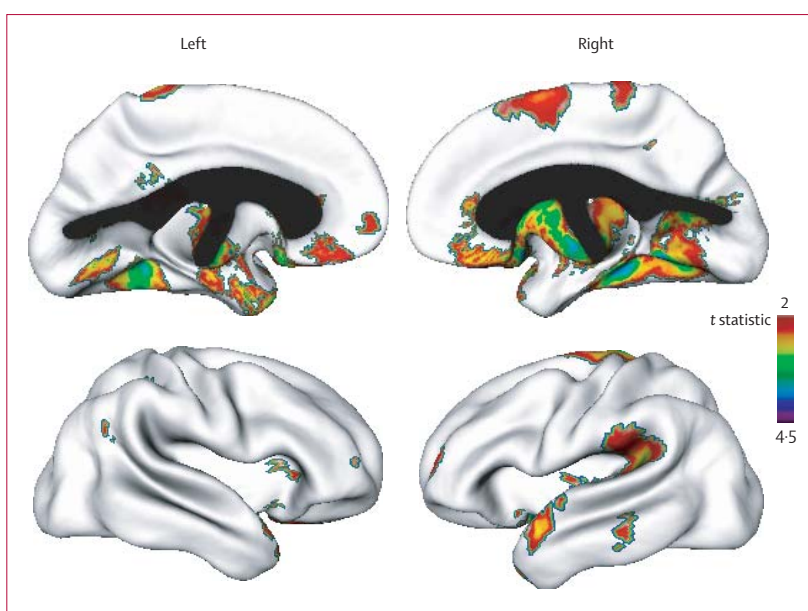


**Figure 2: t statistical map of thinning in  $\epsilon 4$  carriers compared with non-carriers**

Differences in cortical thickness between  $\epsilon 4$  carriers and non-carriers were projected onto a brain template (top panels are medial views, bottom panels are lateral views). Regions where  $\epsilon 4$  carriers had a thinner cortex are indicated (at  $t > 2$ ,  $p < 0.05$ ); regions in yellow, green, and blue remained significant after adjustment for multiple comparisons.

Much the same pattern of results was found when analyses were confined to white, non-hispanic individuals and when analyses were confined to singleton births only (webappendix 4 and webfigure 5). With the exception of a small region in the postcentral gyrus, there was no significant interaction between sex and genotype group, and no significant three way interaction between sex, genotype and group and age (data not shown). Analyses in stereotaxic space showed a very similar distribution to the changes noted in native space, with  $\epsilon 4$  carriers having a significantly thinner medial temporal cortex, extending anteriorly to the posterior orbitofrontal cortex. Changes in the parahippocampal regions were less pronounced. In stereotaxic space, as in native space, there were only sparse group differences between  $\epsilon 4$  carriers and non-carriers throughout the remaining frontal, parietal, lateral temporal, and occipital cortex.

Cortical development did not differ between  $\epsilon 4$  carriers and non-carriers (neither the  $\epsilon 2$  carriers nor the  $\epsilon 3$  homozygotes) of different ages in the regions of interest (figure 3). Throughout the remainder of the cortex, the effect of genotype on cortical thickness did not vary significantly with age, with the exception of a small region in the left middle temporal/angular gyrus; however, the differences in thickness in this region did not remain significant after adjustment for multiple comparisons (webappendix 2).

### Discussion

Our data suggest that children and adolescents possessing the  $\epsilon 4$  allele of the *APOE* gene have a thinner cortex in

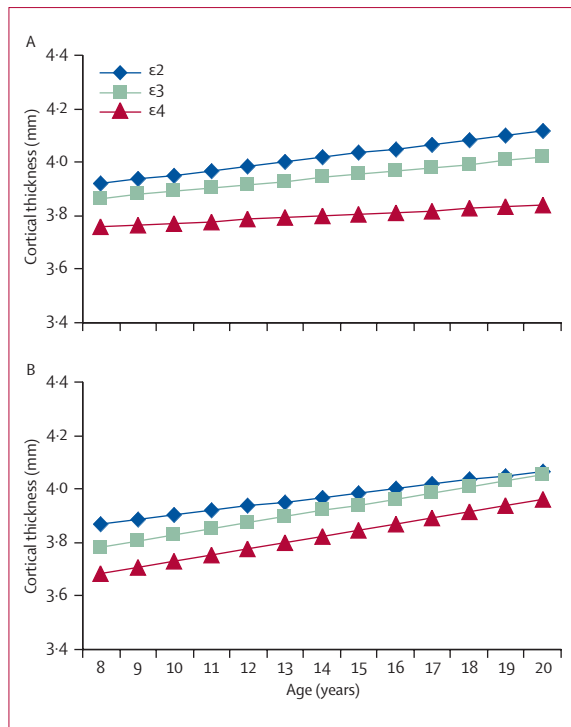


**Figure 3:** Cortical thickness in the entorhinal cortical regions of interest at different ages

Left (A) and right (B) entorhinal cortical region. Change in thickness does not differ by APOE genotype (all pairwise comparisons for difference in slopes  $p > 0.5$ ).  $\epsilon 2 = \epsilon 2$  carriers.  $\epsilon 3 = \epsilon 3$  homozygotes.  $\epsilon 4 = \epsilon 4$  carriers.

the entorhinal region—the site of the earliest changes associated with Alzheimer’s disease—than do individuals without this allele. We also noted a stepwise increase in cortical thickness in the entorhinal cortex moving from the thinnest cortex in  $\epsilon 4$  carriers, through an intermediate thickness for  $\epsilon 3$  homozygotes, with carriers of the  $\epsilon 2$  allele having the thickest cortex. This linear effect was also noted in small regions of the medial temporal and posterior-medial orbitofrontal cortex; these regions are also severely affected in Alzheimer’s disease<sup>29</sup> and have a marked cytoarchitectural similarity with the entorhinal cortical regions.<sup>42</sup> There was no evidence of genotypic effects throughout the remaining cortex. The neuroanatomic effects seemed to be fixed and non-progressive, with no evidence of differential rates of change in young  $\epsilon 4$  carriers.

The thinner cortex in  $\epsilon 4$  carriers could represent a genetically determined neuroanatomic property—in other words, a neural endophenotype—that renders carriers more susceptible to degenerative changes later in life. Thus, by virtue of possessing a thinner cortex in certain key regions, less cortical thinning might be required in  $\epsilon 4$  carriers before a critical anatomical threshold is passed, which manifests as cognitive decline. This hypothesis can be best tested through longitudinal studies of the healthy ageing adult population.

We can only speculate on cellular events that may underlie change in cortical thickness, but these probably include alterations in synaptic connections and changing myelination of the peripheral cortical neuropil.<sup>43–45</sup> The thinner cortex in  $\epsilon 4$  carriers might also indicate early changes of pre-symptomatic Alzheimer’s disease—eg, the presence of neurofibrillary tangles—which can induce metabolic decline leading to neuronal loss and thus perhaps cortical thinning.<sup>46,47</sup>

We assessed the effects of possession of the  $\epsilon 4$  allele in a large group of healthy children by use of a fully automated measure of cortical thickness. These methods have been used to characterise cortical change in adults with Alzheimer’s disease.<sup>9,48</sup> The technique has proved suitable for charting development change in healthy children and is sensitive to the effects of genotypic and cognitive variation on cortical change.<sup>49</sup> Exactly the same analytical tools were used by Lerch and colleagues,<sup>9</sup> in adults who showed that cortical thinning of parahippocampal cortex in Alzheimer’s disease was an order of magnitude greater (at 1.25 mm) than the thinning we found in  $\epsilon 4$  carriers in the right parahippocampal region (0.13 mm). However, direct comparison of these studies is complicated by differences in the scanning sequences, use of distinct adult and paediatric templates to define the regions of interest, and age-related differences in the healthy entorhinal cortex, which increases in thickness into adulthood.

We did not find a genotype effect on IQ in our cohort, but because we did not include tests of memory and learning, we cannot exclude the possibility that there could be associations with  $\epsilon 4$  carrier status and these cognitive functions. Nonetheless, the finding that altered neural substrate in childhood and adolescence was not associated with any difference in intellectual ability is in line with previous studies, which show little or no cognitive effects of possession of the  $\epsilon 4$  allele in children and young adults.<sup>50–52</sup> Indeed some studies find protective effects of the  $\epsilon 4$  allele in early development, with reports of higher perinatal survival rates and protection of cognitive development in the face of illness.<sup>53,54</sup> The deleterious cognitive effects associated with possession of an  $\epsilon 4$  allele are thus more apparent in later life. Thus the thinner cortex of  $\epsilon 4$  carriers might be best conceptualised as a phenotypic variant, rather than a pathological change, which is essentially harmless in childhood and adolescence, but could contribute in later life to the development of cognitive decline.

Our finding of a thicker cortex in  $\epsilon 2$  carriers could contribute to the explanation of the so-called protective effects of the  $\epsilon 2$  allele. Several cellular models have been proposed to explain the effects of this allele, such as its ability to block the effects of amyloid  $\beta$  accumulation.<sup>55,56</sup> Here we show evidence for a neuroanatomic effect.

There was no evidence of significantly different cortical development over time related to  $\epsilon 4$  allele status, and thus no support for a concept of accelerated cortical decline

present in childhood. This finding is perhaps unsurprising in a paediatric cohort, since progressive change would be more likely to have manifest cognitive effects. Although an effect could have been missed due to attrition biases, this is made less likely by the similar proportions of individuals in each genotype group who had repeated neuroanatomic imaging and the baseline similarity between those with one scan compared with those with repeated scans. The ethnic heterogeneity, high socioeconomic status, above average IQ, and large proportion of twin births could limit the generalisability of the results, although we note that the results held after controlling for these variables. Although the algorithm we used and its derivatives currently lack validation against manual measurements of the medial temporal lobes, the techniques can accurately extract the cortical surfaces of a phantom brain, detect simulated thinning of the temporal cortex, and capture the neuropathologically established pattern of progression of cortical degeneration within the medial temporal lobes in Alzheimer's disease.<sup>9,36,57,58</sup>

In summary, our data indicate that possession of an  $\epsilon 4$  allele could be associated with a cortical endophenotype, characterised by a thinner entorhinal cortex, which seems to be cognitively silent in childhood, but could render individuals more prone to the later development of Alzheimer's disease.

#### Contributors

PS designed the study, analysed the neuroimaging data, and wrote the manuscript with JG and JR. DG conducted statistical analyses. KNT and ABR did the genotyping. JL and AE developed the analytic tools software. JCP designed the entorhinal templates. The study was directed by JG and JR. LC was the data manager.

#### Conflict of interest

We have no conflicts of interest.

#### Acknowledgments

The research was funded by the Intramural Research Program at the National Institutes of Health. The authors thank the young people who took part in the study and their families.

#### References

- Braak H, Braak E. Neuropathological staging of Alzheimer-related changes. *Acta Neuropathologica* 1991; **82**: 239–59.
- Braak H, Braak E, Yilmazer D, de Vos RA, Jansen EN, Bohl J. Pattern of brain destruction in Parkinson's and Alzheimer's diseases. *J Neural Transm* 1996; **103**: 455–90.
- Ghebremedhin E, Schultz C, Braak E, Braak H. High frequency of apolipoprotein E epsilon4 allele in young individuals with very mild Alzheimer's disease-related neurofibrillary changes. *Exp Neurol* 1998; **153**: 152–55.
- Krasuski JS, Alexander GE, Horwitz B, et al. Volumes of medial temporal lobe structures in patients with Alzheimer's disease and mild cognitive impairment (and in healthy controls). *Biol Psychiatry* 1998; **43**: 60–68.
- Callen DJ, Black SE, Gao F, Caldwell CB, Szalai JP. Beyond the hippocampus: MRI volumetry confirms widespread limbic atrophy in AD. *Neurology* 2001; **57**: 1669–74.
- Xu Y, Jack CR Jr, O'Brien PC, et al. Usefulness of MRI measures of entorhinal cortex versus hippocampus in AD. *Neurology* 2000; **54**: 1760–67.
- Juottonen K, Laakso MP, Partanen K, Soininen H. Comparative MR analysis of the entorhinal cortex and hippocampus in diagnosing Alzheimer disease. *AJNR Am J Neuroradiol* 1999; **20**: 139–44.
- Thompson PM, Hayashi KM, Sowell ER, et al. Mapping cortical change in Alzheimer's disease, brain development, and schizophrenia. *Neuroimage* 2004; **23** (suppl 1): S2–18.
- Lerch JP, Pruessner JC, Zijdenbos A, Hampel H, Teipel SJ, Evans AC. Focal decline of cortical thickness in Alzheimer's disease identified by computational neuroanatomy. *Cerebral Cortex* 2005; **15**: 995–1001.
- Scahill RI, Schott JM, Stevens JM, Rossor MN, Fox NC. Mapping the evolution of regional atrophy in Alzheimer's disease: Unbiased analysis of fluid-registered serial MRI. *Proc Natl Acad Sci USA* 2002; **99**: 4703–07.
- de Leon MJ, Convit A, Wolf OT, et al. Prediction of cognitive decline in normal elderly subjects with 2-[(18)F]fluoro-2-deoxy-D-glucose/positron-emission tomography (FDG/PET). *Proc Natl Acad Sci USA* 2001; **98**: 10966–71.
- de Toledo-Morrell L, Stoub TR, Bulgakova M, et al. MRI-derived entorhinal volume is a good predictor of conversion from MCI to AD. *Neurobiol Aging* 2004; **25**: 1197–203.
- Corder EH, Saunders AM, Strittmatter WJ, et al. Gene dose of apolipoprotein E type 4 allele and the risk of Alzheimer's disease in late onset families. *Science* 1993; **261**: 921–23.
- Farrer LA, Cupples LA, Haines JL, et al. Effects of age, sex, and ethnicity on the association between apolipoprotein E genotype and Alzheimer disease. A meta-analysis. APOE and Alzheimer Disease Meta Analysis Consortium. *JAMA* 1997; **278**: 1349–56.
- Scarmeas N, Habeck CG, Hilton J, et al. APOE related alterations in cerebral activation even at college age. *J Neurol Neurosurg Psychiatry* 2005; **76**: 1440–44.
- Scarmeas N, Anderson KE, Hilton J, et al. APOE-dependent PET patterns of brain activation in Alzheimer disease. *Neurology* 2004; **63**: 913–15.
- Bookheimer SY, Strojwas MH, Cohen MS, et al. Patterns of brain activation in people at risk for Alzheimer's disease. *N Engl J Med* 2000; **343**: 450–56.
- Smith CD, Andersen AH, Kryscio RJ, et al. Women at risk for AD show increased parietal activation during a fluency task. *Neurology* 2002; **58**: 1197–202.
- Small GW, Ercoli LM, Silverman DH, et al. Cerebral metabolic and cognitive decline in persons at genetic risk for Alzheimer's disease. *Proc Natl Acad Sci USA* 2000; **97**: 6037–42.
- Reiman EM, Chen K, Alexander GE, et al. Correlations between apolipoprotein E epsilon4 gene dose and brain-imaging measurements of regional hypometabolism. *Proc Natl Acad Sci USA* 2005; **102**: 8299–302.
- Teter B, Ashford JW. Neuroplasticity in Alzheimer's disease. *J Neurosci Res* 2002; **70**: 402–37.
- Buttini M, Orth M, Bellosta S, et al. Expression of human apolipoprotein E3 or E4 in the brains of Apoe<sup>-/-</sup> mice: isoform-specific effects on neurodegeneration. *J Neurosci* 1999; **19**: 4867–80.
- Teasdale GM, Murray GD, Nicoll JA. The association between APOE epsilon4, age and outcome after head injury: a prospective cohort study. *Brain* 2005; **128**: 2556–61.
- Blackman JA, Worley G, Strittmatter WJ. Apolipoprotein E and brain injury: Implications for children. *Dev Med Child Neurol* 2005; **47**: 64–70.
- Ganguli M, Chandra V, Kambh MI, et al. Apolipoprotein E Polymorphism and Alzheimer disease: The Indo-US Cross-National Dementia Study. *Arch Neurol* 2000; **57**: 824–30.
- Katzman R, Zhang MY, Chen PJ, et al. Effects of apolipoprotein E on dementia and aging in the Shanghai Survey of Dementia. *Neurology* 1997; **49**: 779–85.
- Qiu C, Kivipelto M, Aguero-Torres H, Winblad B, Fratiglioni L. Risk and protective effects of the APOE gene towards Alzheimer's disease in the Kungsholmen project: variation by age and sex. *J Neurol Neurosurg Psychiatry* 2004; **75**: 828–33.
- Wilson RS, Bienias JL, Berry-Kravis E, Evans DA, Bennett DA. The apolipoprotein E [varepsilon]2 allele and decline in episodic memory. *J Neurol Neurosurg Psychiatry* 2002; **73**: 672–77.
- Van Hoesen GW, Parvizi J, Chu C-C. Orbitofrontal cortex pathology in Alzheimer's disease. *Cereb Cortex* 2000; **10**: 243–51.
- Giedd JN, Snell JW, Lange N, et al. Quantitative magnetic resonance imaging of human brain development: ages 4–18. *Cereb Cortex* 1996; **6**: 551–59.

- 31 Collins DL, Neelin P, Peters TM, Evans AC. Automatic 3D intersubject registration of MR volumetric data in standardized Talairach space. *J Comput Assist Tomogr* 1994; **18**: 192–205.
- 32 Sled JG, Zijdenbos AP, Evans AC. A nonparametric method for automatic correction of intensity nonuniformity in MRI data. *IEEE Trans Med Imag* 1998; **17**: 87–97.
- 33 Zijdenbos AP, Forghani R, Evans AC. Automatic “pipeline” analysis of 3-D MRI data for clinical trials: application to multiple sclerosis. *IEEE Trans Med Imag* 2002; **21**: 1280–91.
- 34 MacDonald D, Kabani N, Avis D, Evans AC. Automated 3-D extraction of inner and outer surfaces of cerebral cortex from MRI. *Neuroimage* 2000; **12**: 340–56.
- 35 Kim JS, Singh V, Lee JK, et al. Automated 3-D extraction and evaluation of the inner and outer cortical surfaces using a Laplacian map and partial volume effect classification. *Neuroimage* 2005; **27**: 210–21.
- 36 Lerch JP, Evans AC. Cortical thickness analysis examined through power analysis and a population simulation. *Neuroimage* 2005; **24**: 163–73.
- 37 Pruessner JC, Kohler S, Crane J, et al. Volumetry of temporopolar, perirhinal, entorhinal and parahippocampal cortex from high-resolution MR images: considering the variability of the collateral sulcus. *Cereb Cortex* 2002; **12**: 1342–53.
- 38 Collins DL, Holmes CJ, Peters TM, Evans AC. Automatic 3-D model-based neuroanatomical segmentation. *Human Brain Mapping* 1995; **3**: 190–208.
- 39 Pinheiro JC, Bates DM. Mixed-effects models in S and S-PLUS. New York: Springer, 2000.
- 40 Benjamini Y, Hochberg Y. Controlling the false discovery rate: a practical and powerful approach to multiple testing. *J R Stat Soc Ser B* 1995; **57**: 289–300.
- 41 Genovese CR, Lazar NA, Nichols T. Thresholding of statistical maps in functional neuroimaging using the false discovery rate. *Neuroimage* 2002; **15**: 870–78.
- 42 Ongur D, Ferry AT, Price JL. Architectonic subdivision of the human orbital and medial prefrontal cortex. *J Comp Neurol* 2003; **460**: 425–49.
- 43 Sowell ER, Thompson PM, Leonard CM, Welcome SE, Kan E, Toga AW. Longitudinal mapping of cortical thickness and brain growth in normal children. *J Neurosci* 2004; **24**: 8223–31.
- 44 Yakovlev PI, Lecours AR. The myelinogenetic cycles of regional maturation of the brain. In: Minokowski A, ed. Regional development of the brain in early life. Oxford: Blackwell Scientific, 1967.
- 45 Huttenlocher PR, Dabholkar AS. Regional differences in synaptogenesis in human cerebral cortex. *J Comp Neurol* 1997; **387**: 167–78.
- 46 Gomez-Isla T, Hyman BT. Neuropathological changes in normal aging, mild cognitive impairment, and Alzheimer’s disease. In: Petersen RC, ed. Mild cognitive impairment: aging to Alzheimer’s disease, 2003.
- 47 Grignon Y, Duyckaerts C, Bannic M, Hauw JJ. Cytoarchitectonic alterations in the supramarginal gyrus of late onset Alzheimer’s disease. *Acta Neuropathol (Berl)* 1998; **95**: 395–406.
- 48 Kabani N, Le Goualher G, MacDonald D, Evans AC. Measurement of cortical thickness using an automated 3-D algorithm: a validation study. *Neuroimage* 2001; **13**: 375–80.
- 49 Shaw P, Greenstein D, Lerch J, et al. Intellectual ability and cortical development in children and adolescents. *Nature* 2006; **440**: 676–79.
- 50 Turic D, Fisher PJ, Plomin R, Owen MJ. No association between apolipoprotein E polymorphisms and general cognitive ability in children. *Neurosci Lett* 2001; **299**: 97–100.
- 51 Small BJ, Rosnick CB, Fratiglioni L, Backman L. Apolipoprotein E and cognitive performance: a meta-analysis. *Psychol Aging* 2004; **19**: 592–600.
- 52 Deary IJ, Whalley LJ, et al. The influence of the epsilon 4 allele of the apolipoprotein E gene on childhood IQ, nonverbal reasoning in old age, and lifetime cognitive change. *Intelligence* 2003; **31**: 85–92.
- 53 Becher JC, Keeling JW, McIntosh N, Wyatt B, Bell J. The distribution of apolipoprotein E alleles in Scottish perinatal deaths. *J Med Genet* 2006; **43**: 414–18.
- 54 Oria RB, Patrick PD, Zhang H, et al. APOE4 protects the cognitive development in children with heavy diarrhea burdens in northeast Brazil. *Pediatr Res* 2005; **57**: 310–16.
- 55 Lee G, Pollard HB, Arispe N. Annexin 5 and apolipoprotein E2 protect against Alzheimer’s amyloid-beta-peptide cytotoxicity by competitive inhibition at a common phosphatidylserine interaction site. *Peptides* 2002; **23**: 1249–63.
- 56 Pedersen WA, Chan SL, Mattson MP. A mechanism for the neuroprotective effect of apolipoprotein E: isoform-specific modification by the lipid peroxidation product 4-hydroxynonenal. *J Neurochem* 2000; **74**: 1426–33.
- 57 Lee JK, Lee JM, Kim JS, Kim IY, Evans AC, Kim SI. A novel quantitative cross-validation of different cortical surface reconstruction algorithms using MRI phantom. *Neuroimage* 2006; **31**: 572–84.
- 58 MacDonald D, Kabani N, Avis D, Evans AC. Automated 3-D extraction of inner and outer surfaces of cerebral cortex from MRI. *Neuroimage* 2000; **12**: 340–56.